Int. J. Nano Dimens., 14 (4): 366-372, Autumn 2023

ORIGINAL ARTICLE

Microwave assisted synthesis of rod-shaped Copper Oxide microparticles and study of their bactericidal effects on *Bacillus subtilis*

Nikhil Parasar [1], Bidhan Mohanta [1,*], Abu Barkat Mohammad Gulzar [2], Pranab Behari Mazumder [2]

[1] Department of Physics, Assam University, Silchar, India
[2] Department of Biotechnology, Assam University, Silchar, India

Received 20 June 2023; revised 02 August 2023; accepted 12 August 2023; available online 15 August 2023

Abstract

Bactericidal effect of copper oxide is still a growing area of research even though a lot of experiments have been carried out by the researchers. The present work was designed to explore structural and optical properties of micro-size copper oxide particles (μCuO) synthesized using microwave irradiation. Synthesized samples were characterized with ultraviolet-visible spectroscopy, Fourier transform infrared spectroscopy, x-ray diffraction and scanning electron microscopy. Scanning electron micrographs revealed the formation of rod-shaped copper oxide in micron size. X-ray diffraction pattern showed the synthesized microparticles are in monoclinic phase. Solutions of μCuO with various concentrations from 1% to 15% were prepared using dimethyl sulfoxide for the antibacterial study. Starting from 2% concentration, μCuO started to produce a good inhibition zone around the *Bacillus subtilis* bacteria. The prepared μCuO displayed splendid results in bactericidal activity against *Bacillus subtilis* bacteria. Higher concentrations of the μCuO showed strong action against bacterial growth. Micro-size copper oxide can also be used as an antibacterial agent like nano-size copper oxide.

Keywords: *Antibacterial; FTIR; Microstructure; Rapid Synthesis; X-ray Techniques.*

How to cite this article

Parasar N., Mohanta B., Barkat Mohammad Gulzar A., Behari Mazumder P. Microwave assisted synthesis of rod-shaped Copper Oxide microparticles and study of their bactericidal effects on Bacillus subtilis. Int. J. Nano Dimens., 2023; 14(4): 366-372.

INTRODUCTION

Many experiments for bactericidal effects have been done with various metal oxides such as TiO_2, ZnO, and SiO_2 etc. [1]. When metal oxide reacts with water, it produces highly reactive species such as superoxide, hydroxyl radical, and hydrogen peroxide and these species can inhibit bacterial growth [2]. Several bacteria, fungi, and viruses have become resistant to available nanomaterials. Moreover, new microbial species are naturally evolving. That is why; there still remains a requirement for developing strong antibacterial material [3]. One of the most used metal oxides for bactericidal effects is copper oxide. Out of the various forms of copper oxide, cupric oxide (CuO) is more stable and hence can be used as a good bactericidal agent [2]. From previous reports, it is seen that CuO NPs exhibit strong antibacterial activity against a wide range of gram positive and gram negative bacteria. But some bacteria such as *S. aureus (+)* and *B. subtilis (+)* are found to be less sensitive to CuO NPs [1].

The size and shape of the particles have a promising impact on the microbial-resistant based devices and also in the therapeutic agents with antibacterial, antioxidant, anticancer and drug-delivery properties [4].

The cell wall constituents of the bacteria are sensitive to the differently shaped CuO NPs. Sheet shaped CuO are reported to be active against gram positive bacteria, while spherical CuO are more

* Corresponding Author Email: *mbidhan@gmail.com*

effective against gram negative bacteria [1]. That is why copper oxide nanoparticles have an ample use in the biomedical domain.

CuO particles of smaller sizes depict drastically different physical and chemical properties in comparison to their bulk. The preparation of micro or nano-size CuO can be carried out by various methods such as sol-gel, co-precipitation etc. [5-6]. Different sizes and shapes can be achieved via several methods such as, sonochemical [7], electrochemical methods [8], etc. CuO particles have promising applications in catalytic activity, antibacterial effects etc. It is seen that nanostructures with smaller sizes, narrower size distributions and higher degree of crystallization could be obtained using microwave (MW) heating rather than using conventional heating. Microwave as a heating source has the advantage of fast reaction rate, higher reproducibility, better product purity, higher yields, and scalability compared to conventional heating [9].

Copper nanomaterials are well established as antibacterial agents [10], However rampant use of nanoparticles pose a threat to the environment because these can easily assimilate in human or animal bodies and consequently interaction with their body cells can cause significant damage. Whereas, for micro-size particles, there is a lesser chance of causing environmental damage because, of their have larger size. Studies on the applications of CuO particles largely pertain to their nano forms, whereas reports on the micro-sized particles are almost non-existent. Thus, our endeavor is to check the bactericidal effect of micro-size CuO. *Bacillus subtilis* was taken for this study.

EXPERIMENTAL

Materials

Copper (II) acetate monohydrate [$Cu(CH_3COO)_2.H_2O$, 99.9%] was purchased from Sigma-aldrich, Merck and sodium hydroxide [NaOH, 99.5%] was purchased from Thermo Fisher Scientific cooperation. All chemicals are of analytical grade. De-ionized water was used for preparing all the solutions during the experiment.

Preparation of CuO Microparticles

An aqueous solution of 0.5 molar copper acetate of monohydrate and 2.0 molar solution of sodium hydroxide were prepared separately with 50 ml deionized water under rigorous magnetic stirring. The solutions were mixed and stirred to get a transparent solution at room temperature. The mixture was taken in a borosil beaker and placed in a domestic microwave oven of power 800 W and frequency 2.45 GHz. After 5 minutes of microwave irradiation the dark black precipitate was achieved. The precipitate was separated by centrifugation at 3000 rpm for 10 minutes and washed with distilled water and ethanol for several times to eliminate the impurities. The obtained product was dried in air at room temperature for 8 h to get CuO samples.

Characterization Techniques

A Multiskan SkyHigh Microplate UV-Vis Spectrophotometer was used to find the UV-Vis absorption peak and hence to find the band-gap of the synthesized particles. The FT-IR spectra for the synthesized CuO sample were recorded using FTIR Spectrum Two Spectrometer (PerkinElmer) in the range (4000-400) cm^{-1}. For FTIR measurement, the synthesized sample and KBr was taken in a ratio of 1:5 and ground finely with pestle and mortar. Using a hydraulic press thin pallet was prepared to take the measurement. Crystallite size was measured with powder X-ray diffraction (PXRD). Rigaku Ultima IV was used for the PXRD data. CuKα radiation was used in the XRD measurements. The measurements were taken in the 2θ range from 2° to 80° in steps of 10°, with a sampling time of one second per step. Using the Scherrer equation, the crystal size was calculated. Scanning electron microscopy (SEM) was performed using the JEOL-JSM-6390 model to reveal the particle size and the morphology of the sample.

RESULTS AND DISCUSSION

XRD analysis

To identify the crystalline structure and phase of the synthesized material, the powder x-ray diffraction (PXRD) technique was engaged. PXRD is a non-destructive analytical technique for studying detailed structural information of crystallographic materials. X-rays are diffracted at the planes of the crystal, in a material sample. The atomic arrangement is identified by the peaks produced due to constructive interference of the x-rays and the crystalline sample [11]. The XRD pattern of the CuO samples is displayed in Fig. 1(A). The peaks were found at the 2θ values of 32.49°, 35.54°, 38.74°, 48.73°, 53.48°, 58.25°, 61.52°, 66.25°, 69.14°, 75.11° corresponding to the indices (110),

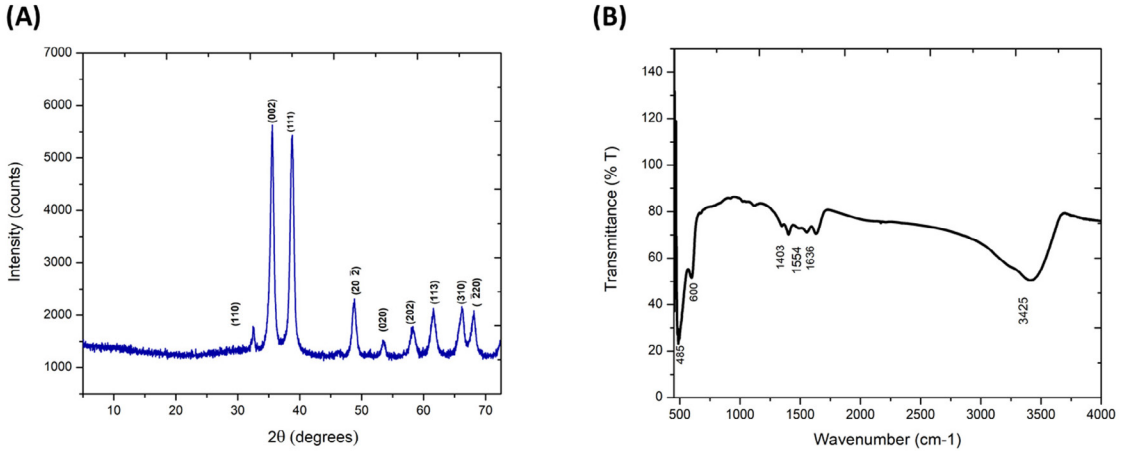

Fig. 1. (A) Powder XRD pattern, (B) FT-IR spectra of the synthesized μCuO.

(002), (111), (202), (020), (202), (113), (310), (220), (222), crystal planes, respectively. These values agree with the monoclinic phase of CuO. There is no peak matching to $Cu(OH)_2$ and Cu_2O in the XRD pattern which confirms the production of pure CuO crystalline phase [12]. Using the Debye-Scherrer formula [13], the average crystallite size of the particles was found to be 67.69 nm.

$$D = \frac{k\lambda}{\beta cos\theta} \quad (1)$$

Where, k is the shape factor (0.9), λ is the wavelength of the applied x-ray, β is the full width at half maximum, θ denotes diffraction angle. The highest peaks (002, 111) were considered for the calculation of the crystallite size. But the equation (1) is best fit for spherical particles, and hence the obtained crystallite size can be considered as an approximate value.

FT-IR spectra analysis

FTIR spectroscopy is a basic tool for spectroscopic study. It is used for the determination of the functional groups present in the material [14]. FT-IR transmission spectrum of the sample is shown in Fig. 1(B). The peaks at 485 cm^{-1} and 600 cm^{-1} are assigned as Cu-O stretching mode vibration [15]. The peaks at 1403, 1554 cm^{-1} are due to the C=O stretching. The sharp peak at 1636 cm^{-1} is attributed to the covalent bond between -OH and CuO. The sharp and broad transmittance peak at 3425 cm^{-1} is due to O-H stretching vibrations of the hydroxyl group of CuO [16].

The functional group available in the sodium hydroxide precursor acts as a reducing agent to reduce the copper (II) metal precursor. Carbonyl and hydroxyl groups are very important for the formation and stabilization of prepared samples to avoid agglomeration [17].

UV-Vis spectra analysis

Various reports on copper oxide have shown that the UV-Visible absorption peak for copper oxide is found in the range (200 – 400) nm. The position of the peak depends on the size of the particles. With increasing size, particles absorb lower energy resulting in red-shift of the absorption peak [3].

UV-Vis absorption data from the sample was taken for the study of optical properties. A 0.05 M solution of the synthesized material diluted to 25 mL distilled water was taken in a quartz cuvette of 1 cm path length. UV-Vis absorption spectrum was measured using a spectrometer. The wavelength vs. absorption graph is shown in Fig. 2(A). The absorption peak was observed at 357 nm wavelength.

The optical band gap of the samples was calculated by Tauc's equation,

$$\alpha h\nu = A\,(h\nu - E_g)^q \quad (2)$$

, where hv is the photon energy, A is a constant and its value depends on the transition probability. Depending upon the nature of transition q value is equal to 2 or ½ for allowed indirect and direct electronic transition respectively. The value of the absorption coefficient (α) can be calculated from the relation:

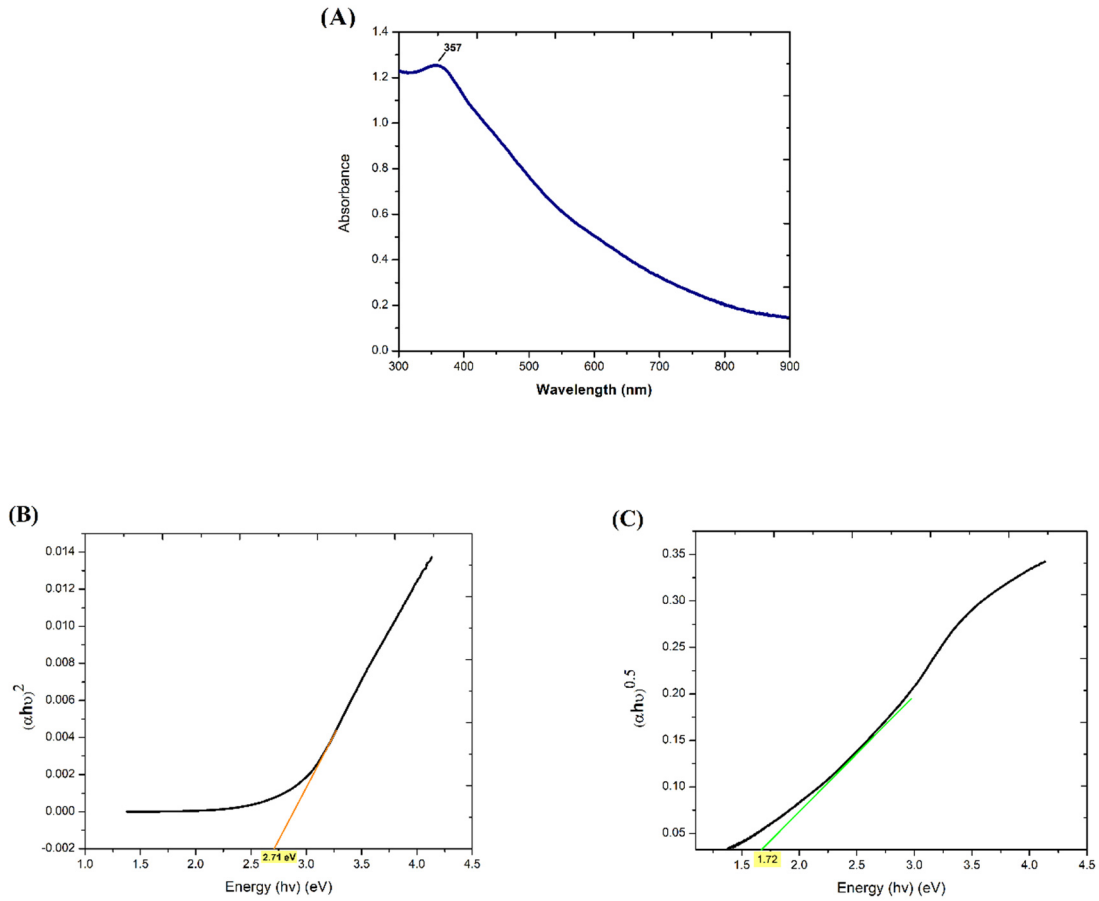

Fig. 2. (A) UV-Vis absorption spectra of the synthesized µCuO, (B) Tauc's plot for direct band gap of the µCuO, (C) Tauc's plot for indirect--band gap of the µCuO.

$$\alpha = 4\pi k/\lambda \quad (3)$$

, where 'k' is the absorption index and 'λ' is the wavelength of the incident photon [18].

Using the above equations, the direct and indirect band gaps of the sample was measured. Tauc's plots were drawn from the UV-Vis absorption data and shown in the Fig. 2(B) and 2(C). As it was seen from the Tauc's plots, the direct band gap of the sample was 2.71 eV and indirect band gap was 1.72 eV.

SEM results

The SEM images of the sample are shown in the Figs. 3(A), 3(B) and 3(C). The images show the surface morphology of the synthesized particles in three different resolutions. It can be seen that the microwave assisted method produced rod-shaped CuO microparticles. Using the SEM data, two histograms are produced to find the average size of the particles as shown in Fig. 4(A), and 4(B). The average diameter and length of the particles are around 5.74 µm and 16.9 µm, respectively. The particle size of the sample is found larger than its crystallite size.

Generally, it is well-known that the particle size is always larger than the crystallite size [19]. However, a vast difference between the sizes of the sample obtained with two different instruments can be seen. This is assumed to happen due to the agglomeration of the particles.

Antibacterial Activities of CuO Microparticles

The antibacterial activities of µCuO were examined against a type of *Bacillus subtilis* bacteria using a well diffusion method. The bacterial isolate was inoculated in the Luria Agar (LA) plate using spread plate method. Wells were made using

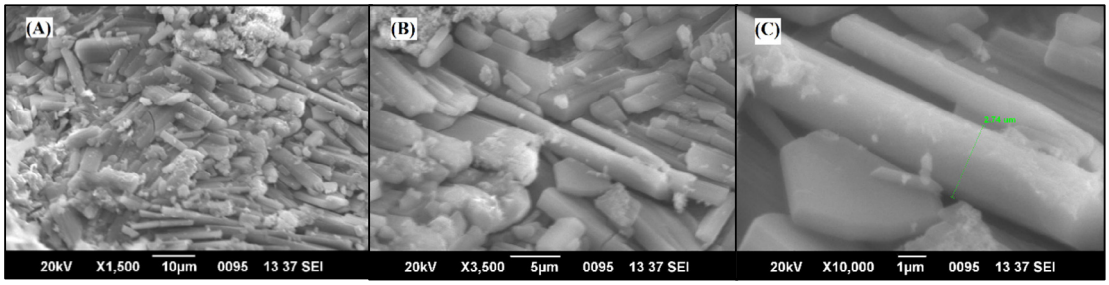

Fig. 3. SEM images of µCuO at different resolutions as (A) x1500, (B) x3500, and (C) x10000.

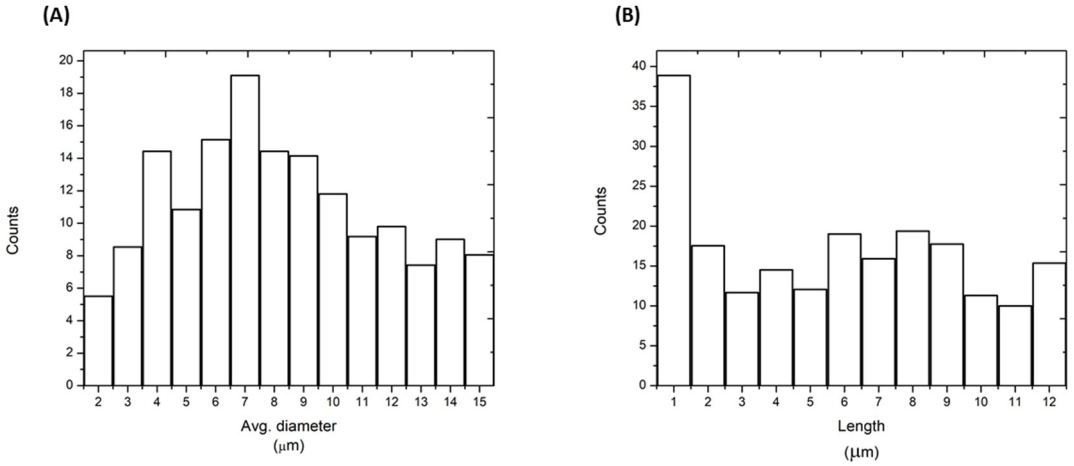

Fig. 4. Histogram prepared from the SEM images for (A) Average diameter, and (B) Average length of µCuO.

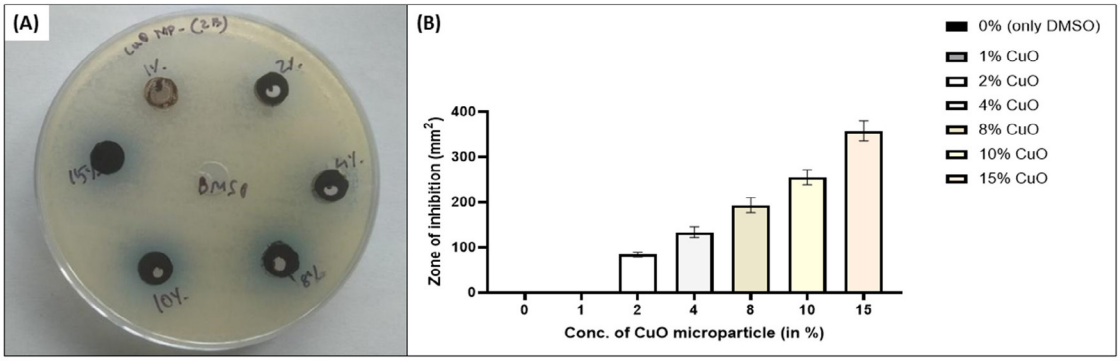

Fig. 5 (A). Bacterial inhibition zones for *Bacillus subtilis* for different concentrations of µCuO; 5 (B) Graphical representations the zone of inhibition of µCuO against *Bacillus subtilis.*

gel punchers. Different concentrations (1%, 2%, 4%, 8%, 10%, and 15%) of µCuO dissolved in DMSO were poured in these wells. The plate was incubated at room temperature (~ 27°C) for 24 h. After incubation, the result was recorded. The experiment was performed in triplicates and the results were presented as mean value ± standard error of mean.

The photographs in Fig. 5 (A) are showing the inhibition zones around the wells and corresponding graphical representation is shown in Fig. 5 (B). It is observed that µCuO are able to inhibit bacterial growth. And the inhibition zones were found to be larger with increasing concentration of µCuO [20]. The area of inhibition zone are calculated for all the concentration and

Table 1. Table representing the area of inhibition zone of µCuO against *Bacillus subtilis*.

Serial number	Conc. of CuO micro-particle (%)	Area of zone of inhibition (mm^2)
1.	DMSO	0
2.	1	0
3.	2	84.03667±5.496667
4.	4	133.2567±11.79243
5.	8	193.4667±16.75667
6.	10	254.9933±16.32668
7.	15	358.14±21.99

± Value = standard error of the mean

described in the Table 1. In this experiment it was found that DMSO has no antibacterial activity and the µCuO exhibited bacterial inhibitory effects at 2% concentration and the zone of inhibition was found to be increased with increasing concentration of µCuO. Highest zone of inhibition was found at concentration of 15% µCuO. However, no antibacterial activity was observed against *Bacillus subtilis* at 1% of µCuO concentration.

CONCLUSIONS

The results show that the method followed was successful in synthesizing CuO in rod-shaped microparticles. The formation of µCuO was confirmed by XRD and SEM analysis. The direct and indirect band gaps of the microparticles were found in the semiconductor range as 2.71 eV and 1.72 eV respectively. The growth of the *Bacillus subtilis* bacteria was successfully inhibited by the µCuO. The result clearly suggests that micro-size CuO rods can be used as antibacterial agents. This result is very significant from the point of view of environmental concerns as microparticles will pose little threat to the ecosystem in comparison to the nanoparticles.

DECLARATIONS

Competing Interest

The authors declare that they have no known competing financial interests or personal relationships that could have appeared to influence the work reported in this paper.

Credit authorship contribution statement

Conceptualization, material preparation, data collection and analysis, editing was done by Nikhil Parasar, Bidhan Mohanta, Abu Barkat Md Gulzar, and Pranab Bihari Mazumder. First draft of the manuscript was written by Nikhil Parasar and all authors commented on the previous version of the manuscript. All authors read and approved the final manuscript.

Funding

This research did not receive any specific grant from funding agencies in the public, commercial, or not-for-profit sectors.

Availability of data and materials

The data that support the findings of this study are available from the corresponding author (B Mohanta) upon reasonable request.

REFERENCES

[1] Laha D., Pramanik A., Laskar A., Jana M., Pramanik P., Karmakar P., (2014), Shape-dependent bactericidal activity of copper oxide nanoparticle mediated by DNA and membrane damage. Mater. Res. Bullet. 59: 185-191. Elsevier BV. https://doi.org/10.1016/j.materresbull.2014.06.024

[2] Maruthapandi M., Saravanan A., Luong J. H. T., Gedanken A., (2020), Antimicrobial properties of polyaniline and polypyrrole decorated with Zinc-doped Copper Oxide microparticles. Polymers. 12: 1286-1291. https://doi.org/10.3390/polym12061286

[3] Bhavyasree P. G., Xavier T. S., (2022), Green synthesized copper and copper oxide based nanomaterials using plant extracts and their application in antimicrobial activity: Review. Current Res. Green and Sustain. Chem. 5: 100249-100253. https://doi.org/10.1016/j.crgsc.2021.100249

[4] Manimaran K., Yanto D. H. Y., Kamaraj C., Selvaraj K., Pandiaraj S., M., Elgorban A., Vignesh S., Kim H., (2023), Eco-friendly approaches of mycosynthesized copper oxide nanoparticles (CuONPs) using Pleurotus citrinopileatus mushroom extracts and their biological applications. Environm. Res. 232: 116319-116323. https://doi.org/10.1016/j.envres.2023.116319

[5] Singh J., Kaur G., Rawat M., (2016), A brief review on synthesis and characterization of copper oxide nanoparticles and its applications. J. Bioelect. Nanotechnol. 1: 9-16. https://doi.org/10.13188/2475-224X.1000003

[6] Khan A., Tariq Z., Malik M. H., (2022), Synthesis, characterization, and photocatalytic applications of novel sword-like copper oxide microparticles. Mate. Lett. 324: 132625-132630. https://doi.org/10.1016/j.matlet.2022.132625

[7] Anandan S., Lee G.-J., Wu J. J., (2012), Sonochemical synthesis of CuO nanostructures with different morphology. Ultrasonics Sonochem. 19: 682-686. https://doi.org/10.1016/j.ultsonch.2011.08.009

[8] Borgohain K., Singh J. B., Rama Rao M. V., Shripathi T., Mahamuni S., (2000), Quantum size effects in CuO

nanoparticles. Phys. Rev. B. 61: 11093-11096. https://doi.org/10.1103/PhysRevB.61.11093

[9] Zhu Y.-J., Chen F., (2014), Microwave-assisted preparation of inorganic nanostructures in liquid phase. Chem. Rev. 114: 6462-6555. https://doi.org/10.1021/cr400366s

[10] Waris A., Din M., Ali A., Ali M., Afridi S., Baset A., Ullah Khan A., (2021), A comprehensive review of green synthesis of copper oxide nanoparticles and their diverse biomedical applications. Inorg. Chem. Communic. 123: 108369-108373. https://doi.org/10.1016/j.inoche.2020.108369

[11] Zhang Y., Xue C., Xue Y., Gao R., Zhang X., (2005), Determination of the degree of deacetylation of chitin and chitosan by X-ray powder diffraction. Carbohyd. Res. 340: 1914-1917. https://doi.org/10.1016/j.carres.2005.05.005

[12] Bekru A. G., Zelekew O. A., Andoshe D. M., Sabir F. K., Eswaramoorthy R., (2021), Microwave-assisted synthesis of CuO nanoparticles using cordia africana lam. Leaf extract for 4-Nitrophenol reduction. J. Nanotech. 2021: 1-12. https://doi.org/10.1155/2021/5581621

[13] Scherrer P., (1912), Bestimmung der inneren struktur und der größe von kolloidteilchen mittels röntgenstrahlen. Kolloidchemie Ein Lehrbuch. 387-409. https://doi.org/10.1007/978-3-662-33915-2_7

[14] Berthomieu C., Hienerwadel R., (2009), Fourier transform infrared (FTIR) spectroscopy. Photosynth. Res. 101: 157-170. https://doi.org/10.1007/s11120-009-9439-x

[15] Jagminas A., Kuzmarskyt J., Niaura G., (2002), Electrochemical formation and characterization of copper oxygenous compounds in alumina template from ethanolamine solutions. Appl. Surf. Sci. 201: 129-137. https://doi.org/10.1016/S0169-4332(02)00649-9

[16] Xia J., Li H., Luo Z., Shi H., Wang K., Shu H., Yan Y., (2009), Microwave-assisted synthesis of flower-like and leaf-like CuO nanostructures via room-temperature ionic liquids. J. Phys. Chem. Solids. 70: 1461-1464. https://doi.org/10.1016/j.jpcs.2009.08.006

[17] Saravanan P., SenthilKannan K., Divya R., Vimalan M., Tamilselvan S., Sankar D., (2020), A perspective approach towards appreciable size and cost-effective solar cell fabrication by synthesizing ZnO nanoparticles from Azadirachta indica leaves extract using domestic microwave oven. J. Mater. Sci: Mater. Electron. 31: 4301-4309. https://doi.org/10.1007/s10854-020-02985-9

[18] Chand P., Gaur A., Kumar A., (2013), Structural, optical and ferroelectric behavior of hydrothermally grown ZnO nanostructures. Superlatt. Microstruc. 64: 331-342. https://doi.org/10.1016/j.spmi.2013.09.038

[19] Wang W.-N., Widiyastuti W., Ogi T., Lenggoro I. W., Okuyama K., (2007), Correlations between crystallite/particle size and photoluminescence properties of submicrometer phosphors. Chem. Mater. 19: 1723-1730. https://doi.org/10.1021/cm062887p

[20] Khodadad H., Hatamjafari F., Pourshamsian Kh., Sadeghi B., (2021), Microwave-assisted synthesis of novel Pyrazole derivatives and their biological evaluation as anti-bacterial agents. Comb. Chem. High Throughput Screen. 24: 695-700. https://doi.org/10.2174/1386207323666201019152206